

Study of reactivity of *p*-cymene ruthenium(II) dimer towards diphenyl-2-pyridylphosphine: Synthesis, characterization and molecular structures of $[(h^6\text{-}p\text{-cymene})\text{RuCl}_2(\text{PPh}_2\text{Py})]$ and $[(h^6\text{-}p\text{-cymene})\text{RuCl}(\text{PPh}_2\text{Py})]\text{BF}_4$

R LALREMPUIA¹, PATRICK J CARROLL² and MOHAN RAO KOLLIPARA^{1,*}

¹Department of Chemistry, North Eastern Hill University, Shillong 793 022, India

²Department of Chemistry, University of Pennsylvania, Philadelphia, PA-19104, USA

e-mail: kmrao@nehu.ac.in

MS received 31 March 2003; revised 8 September 2003

Abstract. The reaction of $[(h^6\text{-}p\text{-cymene})\text{Ru}(\text{mCl})_2\text{Cl}_2]$ with functionalized phosphine viz, diphenyl-2-pyridylphosphine yielded complexes of the type: (a) P-bonded complex $[(h^6\text{-}p\text{-cymene})\text{RuCl}_2(\text{PPh}_2\text{Py})]$ (**1**), (b) P-, N-chelated complex $[(h^6\text{-}p\text{-cymene})\text{RuCl}(\text{PPh}_2\text{Py})]\text{BF}_4$ (**2**) and $[\text{RuCl}_2(\text{PPh}_2\text{Py})_2]$ (**3**) resulting from the displacement of the *p*-cymene ligand. These complexes were characterized by ¹H NMR, ³¹P NMR and analytical data. The structures of complexes **1** and **2** have been confirmed by single crystal X-ray diffraction study. Complex **1** crystallised in triclinic space group $P\bar{1}$ with $a=10.9403$ (3) Å, $b=13.3108$ (3) Å, $c=10.5394$ (10) Å, $\alpha=88.943$ (2)°, $\beta=117.193$ (2)°, $\gamma=113.1680$ (10)°, $Z=2$ and $V=1230.39$ (5) Å³. The complex **2** crystallises in monoclinic space group $P2_1$ with $a=9.1738$ (4) Å, $b=14.0650$ (6) Å, $c=10.7453$ (5) Å, $\beta=106.809$ (1)°, $Z=2$ and $V=1327.22$ (10) Å³.

Keywords. Ruthenium; diphenyl-2-pyridylphosphine; *p*-cymene; X-ray crystallography.

1. Introduction

Arene ruthenium(II) complexes have been the subjects of intense research in the field of organometallic chemistry during recent years.¹ The catalytic activity of these complexes ranges from hydrogen transfer² to ring-closing metathesis.³ Anti tumour activities exhibited by some water-soluble arene ruthenium(II) complexes has also evoked interest in recent years.⁴

We have been interested in the synthesis of arene ruthenium(II) complexes keeping in mind their possible catalytic activity. Pyridylphosphines, in general, continue to induce much interest as being excellent ligands for stabilizing many transition-metal co-ordinations and organometallic complexes.⁵ Diphenyl-2-pyridylphosphine (PPh₂Py) displays numerous ligating modes ranging from P coordination,⁶ P-, N-chelation⁷ and more commonly, P-, N-bridging between two metal centers.⁸ In this paper, we would like to report the synthesis of new com-

plexes where diphenyl 2-pyridylphosphine exhibits bonding modes through (i) P coordination $[(h^6\text{-}p\text{-cymene})\text{RuCl}_2(\text{PPh}_2\text{Py})]$ (**1**), (ii) P-, N-chelating $[(h^6\text{-}p\text{-cymene})\text{RuCl}(\text{PPh}_2\text{Py})]\text{BF}_4$ (**2**) and $[\text{RuCl}_2(\text{PPh}_2\text{Py})_2]$, (**3**). Complex **3** resulted from the displacement of the *p*-cymene ligand from the starting dimer. In order to establish the exact structures, X-ray crystallographic analysis has been carried out for complexes **1** and **2**.

2. Experimental section

All chemicals used were of reagent grade. All reactions were carried out in purified and dried solvents. ¹H NMR spectra were recorded on a Bruker ACF 300 spectrometer. Infrared spectra were taken on a Perkin–Elmer model 983 spectrophotometer using CsI pellets. Elemental analysis was performed in Perkin–Elmer-2400 CHNS/O analyzer. Diphenyl-2-pyridylphosphine (PPh₂Py) was purchased from Aldrich and used as such. $[(h^6\text{-}p\text{-cymene})\text{Ru}(\text{mCl})_2\text{Cl}_2]$ was prepared according to the literature method.⁹

*For correspondence

2.1 Synthesis of $[(h^6-p\text{-cymene})RuCl_2(PPh_2Py)]$ (**1**)

Diphenyl-2-pyridylphosphine (0.043 g, 0.163 mmol) was added to a dichloromethane solution (10 ml) of the complex $[(h^6-p\text{-cymene})Ru(m\text{-Cl})_2Cl_2]$ (0.100 g, 0.163 mmol) and the resulting solution was stirred at room temperature for 1 h. The solvent was reduced to about 2 ml and addition of excess diethylether with vigorous stirring gave the product as a microcrystalline red solid. Yield: 0.148 g, 80%.

Analysis: Calc. for $C_{27}H_{28}NPRuCl_2$: C, 56.98; H, 4.92; N, 2.46%. Found C, 56.94; H, 5.10; N, 2.49%.

1H -NMR ($CDCl_3$, ppm): 8.85 (*d*, $J_{HH} = 4.5$ Hz, 1H), 8.03–7.96 (*m*, 4H), 7.56–7.11 (*m*, 9H), 5.45 (*d*, $J_{HH} = 6.3$ Hz, 2H), 5.32 (*d*, $J_{HH} = 6.3$ Hz, 2H), 2.59 (sept, 1H), 1.68 (*s*, 3H), 0.93 (*d*, $J_{HH} = 6.6$ Hz, 6H).

^{31}P { 1H } NMR ($CDCl_3$, ppm): 21.41 (*s*).

IR (CsI pellet, cm^{-1}): 288 (ν_{Ru-Cl}).

2.2 Synthesis of $[(h^6-p\text{-cymene})RuCl(PPh_2Py)]BF_4$ (**2**) and $[RuCl_2(PPh_2Py)_2]$ (**3**)

The mixture of $[(h^6-p\text{-cymene})Ru(m\text{-Cl})_2Cl_2]$ (0.100 g, 0.163 mmol), diphenyl-2-pyridylphosphine (0.214 g, 0.815 mmol) and NH_4BF_4 (0.085 g, 0.78 mmol) were refluxed in methanol (25 ml). The colour of the solution immediately changed to orange, with some red solid material left at the bottom of the flask, which completely dissolved after refluxing for 3 h to give yellow solution. The solution was then rotary evaporated, extracted with acetone and filtered through a short silica gel column to remove insoluble material. Recrystallisation of the crude product from a mixture of acetone and hexane yielded complex (**2**) as red and complex (**3**) as yellow crystals. These were separated by physical methods.

2.2a Complex 2: Analysis of calc. for $C_{27}H_{28}BClF_4NPRu$: C, 52.25; H, 4.57; N, 2.26%. Found: C, 52.34; H, 4.78; N, 2.32%.

1H NMR ($CDCl_3$, ppm): 9.10 (*d*, $J_{HH} = 5.4$ Hz, 1H), 8.24–8.18 (*m*, 2H), 8.01–7.85 (*m*, 5H), 7.61–7.44 (*m*, 6H), 6.12 (*t*, $J_{HH} = 6.3$ Hz, 2H), 5.90 (*d*, $J_{HH} = 6.0$ Hz, 1H), 5.58 (*d*, $J_{HH} = 6.0$ Hz, 1H), 2.57 (sept, 1H), 1.97 (*s*, 3H), 1.16 (*d*, $J_{HH} = 6.9$ Hz, 3H), 1.05 (*d*, $J_{HH} = 7.2$ Hz, 3H).

^{31}P { 1H } NMR: –11.72 (*s*).

IR (CsI pellet, cm^{-1}): 283 (ν_{Ru-Cl}).

2.2b Complex 3: Analysis of calc. for $C_{34}H_{28}Cl_2Ru$: C, 58.46; H, 4.04; N, 4.00%; Found: C, 58.50; H, 4.25; N, 4.16%.

1H NMR ($CDCl_3$, ppm): 8.55 (*d*, $J_{HH} = 0.3$ Hz, 1H), 8.32 (*t*, $J_{HH} = 7.5$ Hz, 1H), 8.02 (*d*, $J_{HH} = 7.8$ Hz, 1H), 7.86 (*t*, $J_{HH} = 6.0$ Hz, 1H), 7.68 (*t*, $J_{HH} = 7.5$ Hz, 1H), 7.52–7.37 (*m*, 5H), 7.17 (*t*, $J_{HH} = 7.2$ Hz, 2H), and 6.79 (*m*, 2H).

^{31}P { 1H } NMR: 1.50 (*s*).

IR (CsI, cm^{-1}): 280 (ν_{Ru-Cl}).

2.2c Method 2 – Synthesis of $[(h^6-p\text{-cymene})RuCl(PPh_2Py)]BF_4$ (**2**): A mixture of the complex $[(h^6-p\text{-cymene})RuCl_2(PPh_2Py)]$ (**1**) (0.100 g, 0.161 mmol) and NH_4BF_4 (0.042 g, 0.40 mmol) in methanol (15 ml) was stirred at room temperature for 5 h. The clear orange-coloured solution was then rotary evaporated. The residue was extracted with acetone and filtered to remove insoluble material. The filtrate was then reduced to about 1 ml and addition of excess hexane gave orange solid. Yield: 0.085 g, 84%.

2.3 X-ray crystallographic analysis for complexes **1** and **2**

Single crystals suitable for X-ray analysis were grown from dichloromethane/diethylether (complex **1**) and acetone/hexane (complex **2**). X-ray intensity data were collected on a Rigaku R-Axis IIC (Rigaku Mercury CCD for complex **2**) area detector employing graphite-monochromated Mo- K_α radiation ($\lambda = 0.71069$ Å). Indexing was performed from a series of 1° oscillation images with exposures of 200 seconds per frame. A hemisphere of data was collected using 6° oscillation angles with exposures of 150 seconds per frame and a crystal-to-detector distance of 82 mm. Oscillation images were processed using *bioteX*,¹⁰ producing a listing of unaveraged F^2 and $\sigma(F^2)$ values which were then passed to the *teXsan*¹¹ program package for further processing and structure solution on a Silicon Graphics O2 computer. The intensity data were corrected for Lorentz and polarization effects but not for absorption.

The structures were solved by direct methods (SIR92¹²). Refinement was by full-matrix least squares based on F^2 using SHELXL-93.¹³ All reflections were used during refinement (F^2 's that were experimentally negative were replaced by $F^2 = 0$). The weighting scheme used was $w = 1/$

$[S^2(F_0^2) + 0.0682P^2 + 0.8632P]$, where $P = (F_0^2 + 2F_c^2)/3$. Non-hydrogen atoms were refined anisotropically and hydrogen atoms were refined using a 'riding' model. Refinement for complex **1** converged to $R_1 = 0.0416$ and $wR_2 = 0.1089$ for 5351 reflections for which $F > 4\sigma(F)$ and $R_1 = 0.0436$, $wR_2 = 0.1110$ and $GOF = 1.074$ for all 5589 unique, non-zero reflections and 293 variables. Refinement for complex **2** converged to $R_1 = 0.0338$ and $wR_2 = 0.0913$ for 12916 reflections for which $F > 4\sigma(F)$ and $R_1 = 0.0347$, $wR_2 = 0.0927$ and $GOF = 1.090$ for all 13124 unique, non-zero reflections and 329 variables.

Table 1 lists cell information, data collection parameters, and refinement data. Tables 2 and 3 list

bond distances and bond angles of compounds **1** and **2** respectively. Figures 1 and 2 are ORTEP¹⁴ representations of the molecule with 30% probability thermal ellipsoids displayed.

3. Results and discussion

The dinuclear complex $[(\eta^6\text{-}p\text{-cymene})\text{Ru}(\text{m-Cl})_2\text{Cl}_2]$ undergoes bridge cleavage reaction with diphenyl-2-pyridylphosphine yielding neutral P-bonded, cationic P-, N-chelating and neutral P-, N-chelating complexes respectively.

The reaction of $[(\eta^6\text{-}p\text{-cymene})\text{Ru}(\text{m-Cl})_2\text{Cl}_2]$ with one equivalent of the ligand in dichloro-

Table 1. Summary of structure determination of complexes **1** and **2**^a.

Formula	RuC ₂₇ H ₂₈ NPCl ₂	RuC ₂₇ BH ₂₈ NPF ₄ Cl
Formula weight	569.44	620.80
Crystal class	Triclinic	Monoclinic
Space group	$P\bar{1}$ (#2)	$P2_1$ (#4)
Z	2	2
Cell constants		
<i>a</i>	10.9403(3) Å	9.1738(4) Å
<i>b</i>	13.3108(3) Å	14.0650(6) Å
<i>c</i>	10.53940(10) Å	10.7453(5) Å
<i>α</i>	88.943(2)°	
<i>β</i>	117.193(2)°	106.809(1)°
<i>γ</i>	113.1680(10)°	
V	1230.39(5) Å ³	1327.22(10) Å ³
<i>m</i>	9.35 cm ⁻¹	7.97 cm ⁻¹
Crystal size (mm)	0.30 × 0.25 × 0.25	0.27 × 0.25 × 0.24
<i>D</i> _{calc}	1.537 g/cm ³	1.553 g/cm ³
<i>F</i> (000)	580	628
Radiation	Mo-K _α (<i>I</i> = 0.71069 Å)	Mo-K _α (<i>I</i> = 0.71069 Å)
2 θ range	5.02–54.98°	3.96–58.24°
<i>hkl</i> collected	–14 ≤ <i>h</i> ≤ 14; –16 ≤ <i>k</i> ≤ 17; –13 ≤ <i>l</i> ≤ 13	–10 ≤ <i>h</i> ≤ 11; –19 ≤ <i>k</i> ≤ 19; –14 ≤ <i>l</i> ≤ 14
No. of reflections measured	19788	13124
No. of unique reflections	5589 (<i>R</i> _{int} = 0.0254)	13124 (<i>R</i> _{int} = 0.0000)
No. of observed reflections	5351 (<i>F</i> > 4 σ)	12916 (<i>F</i> > 4 σ)
No. of reflections used in refinement	5589	13124
No. of parameters	293	329
<i>R</i> indices (<i>F</i> > 4 σ)	<i>R</i> ₁ = 0.0416 <i>wR</i> ₂ = 0.1089	<i>R</i> ₁ = 0.0338 <i>wR</i> ₂ = 0.0913
<i>R</i> indices (all data)	<i>R</i> ₁ = 0.0436 <i>wR</i> ₂ = 0.1110	<i>R</i> ₁ = 0.0347 <i>wR</i> ₂ = 0.0927
GOF [#] :	1.074	1.090
Final difference peaks (e/Å ³)	+0.701, –0.707	+0.799, –0.809

[#] $R_1 = \frac{\sum |F_o| - \sum |F_c|}{\sum |F_o|}$, $wR_2 = \left\{ \frac{\sum w(F_o^2 - F_c^2)^2}{\sum w(F_o^2)^2} \right\}^{1/2}$, $GOF = \left\{ \frac{\sum w(F_o^2 - F_c^2)^2 / (n - p)}{\sum w(F_o^2)^2} \right\}^{1/2}$, where *n* = the number of reflections and *p* = the number of parameters refined.

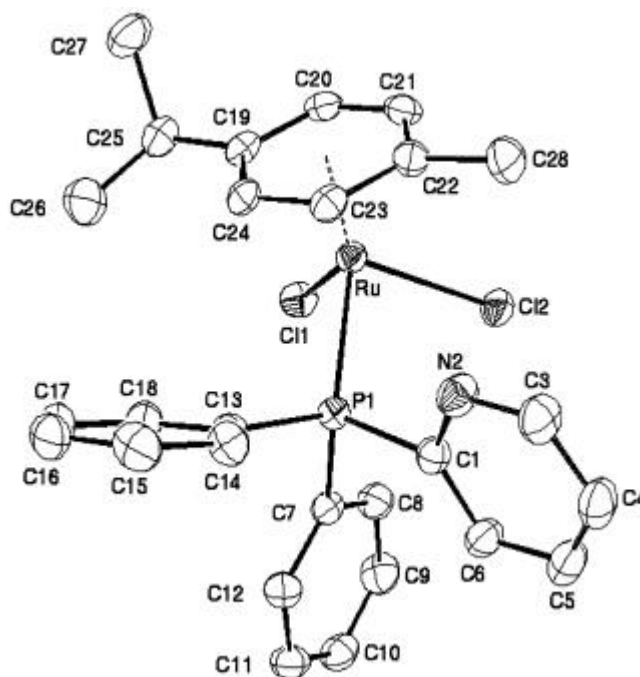
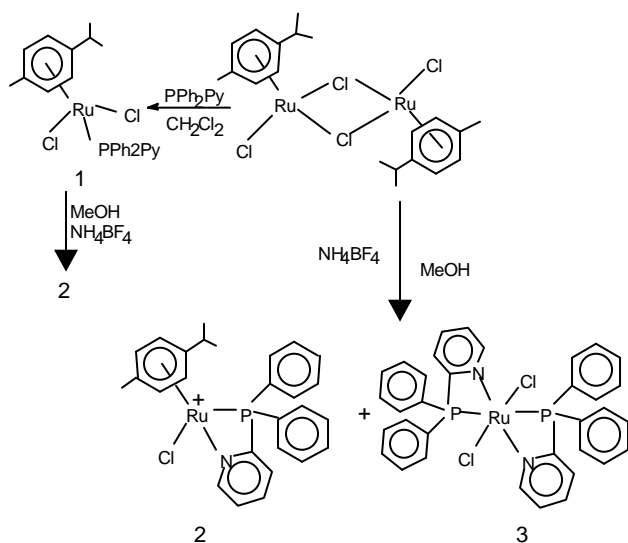
^aThe crystal of complex **2** was found to be twinned by a rotation of 180° about the normal to 301 (twin indexing and processing of twinned data was performed by the TwinSolve^b module of crystal Clear).

^bTwinSolve: C. Swensson, MaxLab, Lund, Sweden, Private Communication.

Table 2. Selected bond lengths (Å) and angles (°) for complex **1**.

Bond lengths (Å)			
Ru–C23	2.160(3)	Ru–Cl11	2.4111(8)
Ru–C19	2.238(3)	C19–C20	1.426(4)
Ru–P1	2.3565(7)	C22–C23	1.405(4)
C19–C24	1.400(4)	Ru–C22	2.217(3)
C21–C22	1.431(5)	Ru–C20	2.251(3)
Ru–C24	2.183(3)	C20–C21	1.378(5)
Ru–C21	2.240(3)	C23–C24	1.430(4)
Ru–Cl2	2.4107(7)		

Bond angles (°)					
C23–Ru–P1	88.99(8)	C24–Ru–P1	94.41(8)	C22–Ru–P1	112.04(9)
C19–Ru–P1	123.52(9)	C21–Ru–P1	149.18(10)	C20–Ru–P1	160.07(9)
C23–Ru–Cl2	119.59(8)	C24–Ru–Cl2	158.00(8)	C22–Ru–Cl2	91.60(8)
C19–Ru–Cl2	151.57(9)	C21–Ru–Cl2	90.84(9)	C20–Ru–Cl2	114.86(9)
P1–Ru–Cl2	84.83(3)	C23–Ru–Cl11	150.85(9)	C24–Ru–Cl11	112.59(8)
C22–Ru–Cl11	157.04(9)	C19–Ru–Cl11	88.18(8)	C21–Ru–Cl11	119.61(10)
C20–Ru–Cl11	92.26(9)	P1–Ru–Cl11	90.90(3)	Cl2–Ru–Cl11	89.41(3)

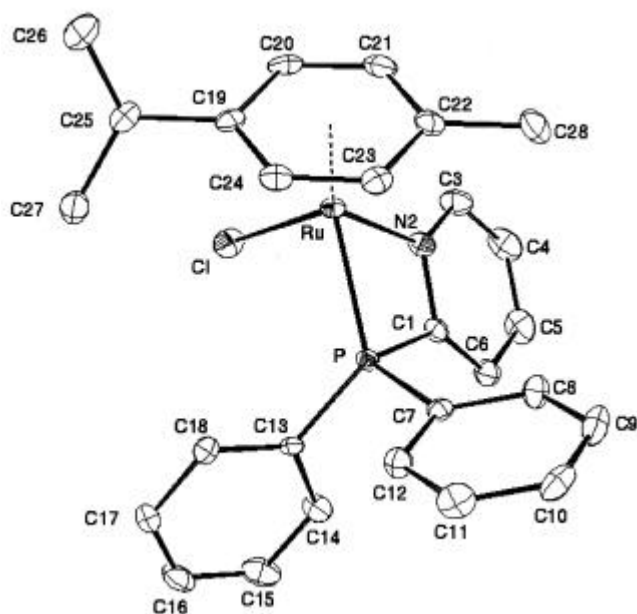
**Figure 1.** Molecular structure of complex [(*h*⁶-*p*-cymene)RuCl₂(PPh₂Py)] (**1**).

methane yielded stable neutral complex [(*h*⁶-*p*-cymene)RuCl₂(PPh₂Py)] (**1**) which is soluble in most of the polar solvents. The spectroscopic data clearly suggest the coordination of the ligand to the metal as evidence from the shift of the phosphorus and protons resonance as compared to the starting materials, but of course without any certain assignment through which atom is bonded to the metal. ¹H NMR spectrum of the complex **1** shows resonance for the phosphine ligand in the aromatic region in the range of 8.85–7.11 ppm. The *p*-cymene signals are well-resolved and exhibit only H–H coupling.

The arene ring protons appear as two sets of doublets at 5.45 and 5.52 ppm while a septet is observed for HC(Me)₂, as found in other *p*-cymene ruthenium complexes. The water peak from the deuterio chloroform solvent obscured CH₃ signal (~1.6 ppm). The

Table 3. Selected bond lengths (Å) and bond angles (°) for complex **2**.

Bond lengths (Å)					
Ru–N2	2.104(2)	Ru–C23	2.166(3)		
Ru–C22	2.207(3)	Ru–C21	2.227(3)		
Ru–C20	2.241(3)	Ru–P	2.3311(7)		
Ru–C24	2.204(3)	P–C1	1.826(3)		
Ru–C19	2.229(3)	C1–C6	1.384(4)		
Ru–C1	2.3970(8)	C5–C6	1.399(5)		
P–C13	1.809(3)	P–C7	1.812(3)		
N2–C1	1.351(4)	N2–C3	1.353(4)		
C3–C4	1.391(5)	C4–C5	1.369(6)		
C19–C24	1.407(4)	C19–C20	1.427(5)		
C20–C21	1.406(5)	C21–C22	1.424(5)		
Bond angles (°)					
N2–Ru–P	67.47(7)	C23–Ru–P	94.25(9)	C24–Ru–P	103.39(7)
C22–Ru–P	112.12(9)	C21–Ru–P	147.06(10)	C19–Ru–P	132.43(9)
C20–Ru–P	169.29(8)	N2–Ru–Cl	83.93(7)	C23–Ru–Cl	152.92(9)
C24–Ru–Cl	115.57(10)	C22–Ru–Cl	159.37(9)	C21–Ru–Cl	121.94(10)
C19–Ru–Cl	91.19(8)	C20–Ru–Cl	95.08(11)	P–Ru–Cl	87.25(3)
N2–Ru–C20	123.15(11)	N2–Ru–C19	159.41(11)	N2–Ru–C21	98.41(11)
N2–Ru–C23	121.58(11)	N2–Ru–C24	158.75(11)	N2–Ru–C22	96.66(11)

**Figure 2.** Molecular structure of complex $[(H^6\text{-}p\text{-cymene})\text{RuCl}(\text{PPh}_2\text{Py})]\text{BF}_4$ (**2**).

protons of isopropyl group ($\text{HC}(\text{Me})_2$) signals appeared as a doublet at 0.93 ppm. The ^{31}P NMR showed one signal at 21.41 ppm due to phosphine ligand, a significant down field shift was observed after coordination to the metal as compared to free

ligand (–3.43 ppm). The far IR spectrum showed a medium intensity band for terminal stretching vibration of $\nu_{\text{Ru-Cl}}$ at 288 cm^{-1} .

The reaction of $[\{(H^6\text{-}p\text{-cymene})\text{Ru}(m\text{-Cl})\}_2\text{Cl}_2]$ with excess of the ligand in methanol yields complexes **2** and **3** in 1:1 ratio as evidenced from ^1H NMR spectrum. These complexes unlike **1** are not soluble in chloroform but are soluble in acetone and dichloromethane. ^1H NMR spectrum of **2** shows different pattern of signals compared to the spectrum of complex **1**, viz. (a) an extra triplet appears for the protons of the *p*-cymene ring. (b) Two doublets are observed at 1.16 and 1.05 ppm for the $\text{HC}(\text{Me})_2$ protons. We have previously reported a similar pattern of signals in the case of *p*-cymene ruthenium(II) Schiff base complexes.¹⁵ This observation could be due to the loss of planarity of the *p*-cymene ligand owing to the steric influence of the rigid P-, N-chelate ligand. The yellow crystals (complex **3**) separated from complex **2** do not show any signals for the *p*-cymene moiety except well-resolved signals in the aromatic region at 8.55–6.76 ppm for phosphine ligand. This type of displacement of the *p*-cymene ring by tertiary phosphines from $[\{(H^6\text{-}p\text{-cymene})\text{Ru}(m\text{-Cl})\}_2\text{Cl}_2]$ is well documented.¹⁶ The ^{31}P -NMR spectrum showed one sharp singlet at 1.50 ppm. The elemental data suggest the compound to be $[\text{RuCl}_2(\text{PPh}_2\text{Py})_2]$ (**3**). The far IR spectrum

taken in CsI showed a band at 280 cm^{-1} , which was assigned to terminal $\nu_{\text{Ru-Cl}}$ stretching mode. The IR data and ^{31}P NMR spectrum suggests that the complex is *trans* product, otherwise one could expect a multiplet for phosphorus and two stretching bands for Ru–Cl.

3.1 Structures of complexes **1** and **2**

An ORTEP view of the complexes **1** and **2** are shown in figures 1 and 2. The complexes exist as half-sandwich complex with the distorted octahedral geometry around the metal centre assuming the *p*-cymene ring occupying three facial sites. The *p*-cymene ligand is *p* bonded to the ruthenium atom with an average Ru–C distance of 2.214 \AA and 2.212 \AA respectively for **1** and **2**. The distance between ruthenium and the chloride ligands are almost same 2.411 and 2.397 \AA . The average C–C bond lengths in the *p*-cymene ring for both the complexes **1** and **2** are 1.411 \AA and 1.416 \AA respectively with alternate short and long C–C bond lengths. The alternate bond lengths are indicative of a contribution from the cyclohexatriene resonance structure to the overall resonance hybrid.¹⁷

In complex **1**, ruthenium atom is directly coordinated to phosphorus atom of the phosphine ligand with a distance of 2.356 \AA . In complex **2**, diphenyl-2-pyridylphosphine ligand is bonded to the ruthenium metal in a chelating fashion forming four-membered ring using both P and N atoms. The bond length of Ru–P is 2.331 \AA , which is shorter, as expected than that of **1** due to the formation of chelate ring. The bond length of Ru–N(2) is 2.104 \AA with in the range of reported compounds. The bond angles P–Ru–Cl(1) and P–Ru–Cl(2) are 90.90 and 84.83 respectively in complex **1** indicating piano stool type structure. The bond angles of P–Ru–Cl and N2–Ru–Cl in complex **3** are 87.25° and 83.93° respectively. The narrow angle of 67.47° for N Ru–P is expected due to the rigidity of the four-member chelating ligand.

4. Supplementary material

Crystallographic data for the structural analysis have been deposited at the Cambridge Crystallographic Data Centre (CCDC), CCDC No. 205909 for complex **1** and 205908 for complex **2** respectively. Copies of this information may be obtained

free of charge from the Director, CCDC, 12 Union Road, Cambridge, CB2 1EZ, UK (fax: +44-1223-336033; e-mail: deposit@ccdc.cam.ac.uk or www: http://www.ccdc.cam.ac.uk).

Acknowledgements

KMR thanks the Department of Science and Technology, New Delhi for financial support. RL thanks the University Grants Commission, New Delhi for financial support.

References

1. Bozec H L, Touchard D and Dixneuf P H 1989 *Adv. Organomet. Chem.* **29** 163
2. Hauser C S, Slugove C, Mereiter K, Schmid R, Kirchner K, Xiao L and Weissensteiner W 2001 *J. Chem. Soc., Dalton Trans.* 2989
3. (a) Fürstner A, Picquet M, Bruneau C and Dixneuf P H 1998 *Chem. Commun.* 1315; (b) Soderberg B C G 2003 *Coord. Chem. Rev.* **241** 147
4. (a) Allardyce C S, Dyson P J, Ellis D J and Heath S L 2001 *Chem. Commun.* 1396; (b) Chen H, Parkinson J A, Parsons S, Coxall R A, Gould R O and Sadler P J 2002 *J. Am. Chem. Soc.* **124** 3064; (c) Aird R E, Cummings J, Ritchie A A, Muir M, Morris R E, Chen H, Sadler P J and Jodrell D I 2002 *Br. J. Cancer* **86** 1652; (d) Morris R E, Aird R E, del S Murdoch P, Chen H, Cummings J, Hughes N D, Parsons S, Parkin A, Boyd G, Jodrell D I and Sadler P J 2001 *J. Med. Chem.* **44** 3616
5. Espinet P and Soulantica K 1999 *Coord. Chem. Rev.* **193–195** 499
6. (a) Xie Y and James B R 1991 *J. Organomet. Chem.* **417** 277; (b) Farr J P, Olmstead M M and Balch A L 1981 *J. Am. Chem. Soc.* **102** 6654; (c) Farr J P, Olmstead M M, Lindsay C H and Balch A L 1981 *Inorg. Chem.* **20** 1182
7. (a) Schutte R P, Rettig S J, Joshi A J and James B R 1997 *Inorg. Chem.* **36** 5809; (b) Casares J A, Espinet P, Hernando R, Iturbe G and Villafane F 1997 *Inorg. Chem.* **36** 44
8. (a) Farr J P, Olmstead M M, Wood F F and Balch A L 1983 *J. Am. Chem. Soc.* **105** 192; (b) Maisonnat A, Farr J P, Olmstead M M, Hunt C T and Balch A L 1982 *Inorg. Chem.* **21** 3961; (c) Olmstead M M, Maisonnat A, Farr J P and Balch A L 1981 *Inorg. Chem.* **20** 4060
9. Bennett M A and Smith A K 1982 *Inorg. Synth.* **21** 74
10. BioteX: A suite of programs for the collection, reduction and interpretation of imaging plate data, Molecular Structure Corporation (1995)
11. teXsan: Crystal Structure Analysis Package, Molecular Structure Corporation (1985 and 1992)
12. SIR92: Altomare A, Burla M C, Camalli M, Cascarano M, Giacovazzo C, Guagliardi A and Polidoro G 1994 *J. Appl. Crystallogr.* **27** 435

13. SHELXL-93: Program for the refinement of crystal structures, Sheldrick, G M 1993 University of Göttingen, Germany
14. 'ORTEP-II: A fortran thermal ellipsoid plot program for crystal structure illustrations'. Johnson C K 1976 ORNL-5138
15. Lalrempuia R, Mohan Rao K and Patrick J Carroll 2003 *Polyhedron* **22** 605
16. Bennett M A and Smith A K 1974 *J. Chem. Soc., Dalton Trans.* 233
17. Lahuerta P, Latorre J, Sanau M, Cotton F A and Schwotzer W 1988 *Polyhedron* **7** 1311